frontiers in Chemistry

ORIGINAL RESEARCH
published: 11 September 2018
doi: 10.3389/fchem.2018.00385

Acetone Sensing Properties and Mechanism of Rh-Loaded WO_3 Nanosheets

Zhilei Qiu[1], Zhongqiu Hua[1], Yan Li[1], Mengjun Wang[1]*, Dan Huang[1], Chen Tian[1], Chensheng Zhang[1], Xuemin Tian[1] and Erping Li[2]*

[1] Tianjin Key Laboratory of Electronic Materials and Devices, School of Electronics and Information Engineering, Hebei University of Technology, Tianjin, China, [2] Key Laboratory of Micro-Nano Electronics and Smart System of Zhejiang Province, Department of Information Science & Electronic Engineering, Zhejiang University, Hangzhou, China

WO_3 nanosheets was prepared by an acidification method and the Rh catalyst was dispersed on the surface of the nanosheets with a wet impregnation method. The morphology of pristine WO_3 and Rh modified WO_3 nanosheets and their responses to acetone gas were studied. According to oxygen adsorption combined with TPR results, the sensing and sensitization mechanism of acetone were discussed. It was found that no visible changes in nanostructures or morphologies were observed in WO_3 nanosheets with Rh, however, the sensor resistance and sensor response were greatly promoted. The basic sensitization mechanism could be caused by the electronic interaction between oxidized Rh and WO_3 surface.

Keywords: WO_3, Rh, acetone, surface modification, gas sensors

OPEN ACCESS

Edited by:
Wen Zeng,
Chongqing University, China

Reviewed by:
Dachi Yang,
Nankai University, China
Guotao Duan,
Institute of Solid State Physics, Hefei Institutes of Physical Science (CAS), China

***Correspondence:**
Zhongqiu Hua
zhongqiuhua@hebut.edu.cn
Mengjun Wang
wangmengjun@hebut.edu.cn

Specialty section:
This article was submitted to Nanoscience, a section of the journal Frontiers in Chemistry

Received: *12 July 2018*
Accepted: *09 August 2018*
Published: *11 September 2018*

Citation:
Qiu Z, Hua Z, Li Y, Wang M, Huang D, Tian C, Zhang C, Tian X and Li E (2018) Acetone Sensing Properties and Mechanism of Rh-Loaded WO_3 Nanosheets Front. Chem. 6:385. doi: 10.3389/fchem.2018.00385

INTRODUCTION

Acetone gas is closely related to people with diabetes. Medical research has shown that there is a significant difference of acetone concentration in the breath for diabetics and healthy people, the former being higher than 1.8 ppm and the latter being below 0.8 ppm (Owen et al., 1982; Natale et al., 2014). Therefore, through the quantitative detection of the acetone concentration in human exhaled gases, it could achieve the purpose of diagnosis and monitoring to the disease condition. Metal oxide semiconductors (MOS) have been widely reported for gas sensors with the significant advantages, such as low cost, simple process and small size (Hübner et al., 2010; Choi et al., 2014). Tungsten trioxide (WO_3) as an n-type semiconductor has become a research hotspot in the detection of VOC gases in recent years (Kanda and Maekawa, 2005; Kadir et al., 2015; Li et al., 2017). The adsorption and reaction of VOC gas on WO_3 surface could change the semiconductor resistance, so the gas response can be improved by adding highly efficient catalytic elements. The introduction of ruthenium (Ru) and silicon (Si) improve the sensitivity of WO_3 to acetone (Righettoni et al., 2010; Li et al., 2018). Further, Rh is known as a highly efficient catalyst to the catalytic reaction of acetone gas (Houtman and Barteau, 1991). It has been reported that Rh loaded SnO_2 and In_2O_3 significantly improve the response of acetone (Kim et al., 2011; Kou et al., 2018). Therefore, this highly efficient catalyst could be also loaded onto WO_3 surface to increase the response to acetone. In this study, the Rh element was uniformly loaded onto the surface of WO_3 nanosheets based on an impregnation approach. This method has been frequently used in our previous work (Li et al., 2018). The experimental results show that the Rh nanoparticles can significantly enhance the response of WO_3 nanosheets to acetone without changing the surface morphology of WO_3 nanosheets. The basic sensitization mechanism of Rh was also analyzed based on experimental results.

EXPERIMENTAL

WO_3 nanosheets was obtained by dropping Na_2WO_4 solution into H_2SO_4 solution (Kida et al., 2009). Aqueous solution of $RhCl_3$ was impregnated with WO_3 (Rh-WO_3) powders and formed a suspension slurry, which was washed by distilled water and dried. Subsequently, the powders were annealed at 500°C in air. Sensor devices were made by the screen-printing technique. The crystal structures were measured by X-ray diffractometer (XRD; D8FOCUS, Germany). The morphology of sample was analyzed using scanning electron microscopy (FE-SEM; Nova Nano SEM 450, FEI, U. S). Nanosheets were also characterized by a transmission electron microscopy (TEM; Tecnai-F20, FEI, U.S). Energy spectrum analysis of materials uses X-ray photoelectron spectroscopy (XPS, Thermo escalab 250Xi, U. S). The catalyst activity was characterized by H_2 temperature programmed reduction (H_2-TPR; TP-5076, China). The experimental procedure of the TPR was descripted in **Figure S1**. Gas sensing tests were carried out by a conventional gas flow apparatus (see **Figure S2**). The gas sample was kept at a constant flow rate of 100 ml/min by mass flow controllers (MFC). The humidity of gas was <20 ppm and temperature of the chamber was about 50°C. The sensor response (S) was defined as $S = R_a/R_g$, where R_a and R_g are the sensor resistance in air and in the presence of target gases.

RESULTS AND DISCUSSION

The morphology of WO_3 nanosheets was characterized by SEM and TEM. **Figures 1A,B** show SEM images of pristine and 1wt.% Rh-WO_3 nanosheets. One can see that the sample powders consisted of a large amount of nanoparticles with a lateral size from dozens to several hundred nanometers. According to SEM images, there were no visible changes observed in pristine WO_3 and Rh modified one. For the results of specific surface area, pristine WO_3 was ∼12 m^2/g and 1wt. %Rh-WO_3 is about 13 m^2/g, which indicts no significant change. **Figure 2** shows TEM images of the pure WO_3 and 1wt.%Rh-WO_3 nanosheets. It was obvious that the sample powder is actually composed of highly irregular plate-like nanosheets. The insert image of **Figure 2A** presents a selected area diffraction (SAD) pattern of pristine WO_3 nanosheets, suggesting that the nanosheets have a good crystal quality. In addition, some white particles with dozens of nm in size were observed in WO_3 surface, as shown in **Figure 2B**. With the help of SAD in **Figure 2C**, these particles were identified as Rh_2O_3 with lattice spacing of 0.26 nm, corresponding to the (110) plane (JCPDS: 25-0707). It was thought that these large particles of Rh_2O_3 could be due to the aggregation of Rh during washing and drying process, which were not effectively removed during the washing process. While the lattice spacing of 0.38 nm in the HRTEM image was belong to monoclinic WO_3 (JCPDS: 43-1035), which was in a good agreement of XRD results (in **Figure S3**).

The chemical state of Rh on WO_3 surface was also analyzed by XPS. **Figure 3A** presents the XPS spectra of W, detection results of binding energy for $W4f_{7/2}$ and $W4f_{5/2}$ being 35.7eV and 37.9eV, respectively, which is in good agreement with W^{6+} (Dupin et al., 2000). **Figure 3B** shows the XPS spectra of Rh3d obtained from 1wt%Rh-WO_3. Among them, the $Rh2d_{5/2}$ peaked at 309.45eV is a typical oxide centered on Rh^{3+}. In addition, the $Rh2d_{3/2}$ located at 314.5eV is also an oxide centered on Rh^{3+} (Kim et al., 2011). Thus, it could be concluded that Rh was present as an oxidized state of Rh_2O_3 on WO_3 surface. Additional with XPS results, the oxidized state of Rh could be also evidenced by H_2-TPR. **Figure 3C** shows the H_2-TPR results of pristine and 1wt%Rh-WO_3 nanosheets. As expected, there was one weak peak around 370°C observed in pristine WO_3 nanosheets indicating a weak consumption of H_2, which may be due to the weak reduction behavior of WO_3 surface at a high temperature (Li et al., 2018). In contrast, large consumptions of H_2 were observed in 1wt%Rh-WO_3, suggesting a strong reduction behavior. There were two overlapped peaks of H_2 consumption at a low temperature around 110°C and the intensities of peaks were relatively high. It was believed that the consumption of H_2 observed at low temperatures could be due to the reduction of Rh_2O_3 and peaks located different temperature

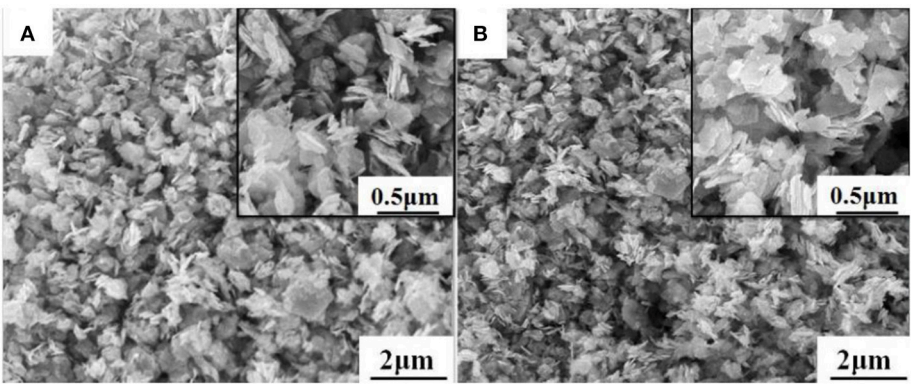

FIGURE 1 | SEM images of **(A)** pure WO_3 nanosheets and **(B)** 1wt%Rh-WO_3 nanosheets.

may be ascribed to different dispersion states of Rh species. There was a broad but weak peak of H_2 consumption at around 450°C, which could be attributable to the weak reduction of WO_3 surface, i.e., surface lattice oxygen (O_L) reacting with H_2 at a high temperature. The reduction behavior of Rh-WO_3 was much stronger than pristine WO_3 indicating that the reactivity of lattice oxygens is slightly promoted by Rh_2O_3 on the surface. We can see significant differences, comparing this reduction behavior with our previous study of Pt-WO_3 nanosheets (in **Figure S4**). At low temperature, Pt-WO_3 produces a negative peak of H_2 desorption. Based on the results of TPR and the resistance behavior under P_{O2}, it is concluded that the main sensitization of Pt-WO_3 may be caused by redox of Pt. nanoparticles (Li et al., 2017). This phenomenon of Rh may cause different sensitization mechanisms.

The sensing properties of pristineWO_3 and Rh-WO_3 nanosheets were characterized with acetone ranging from 0.5 to 10 ppm. **Figure 4A** shows the time dependence of sensor

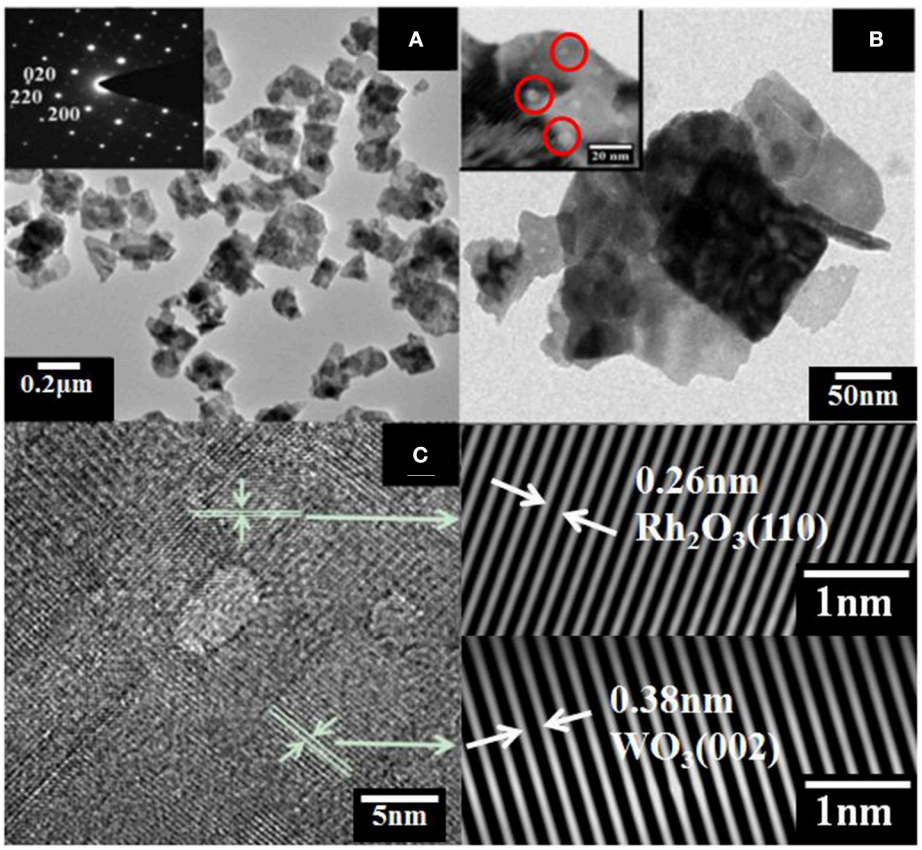

FIGURE 2 | TEM images of **(A)** WO_3 nanosheets insert with selected area diffraction (SAD) pattern, **(B)** 1wt%Rh-WO_3 nanosheets, **(C)** HRTEM image of 1wt%Rh-WO_3 nanosheets and SAD pattern of Rh_2O_3 and WO_3.

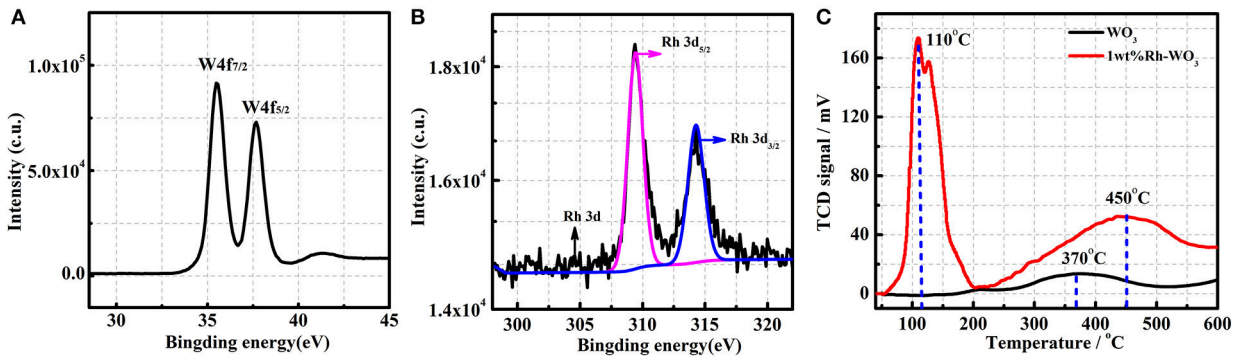

FIGURE 3 | The XPS of 1wt%Rh-WO_3: **(A)** W4f, **(B)** Rh3d, and **(C)** the H_2-TPR patterns of pure WO_3 and 1wt%Rh-WO_3.

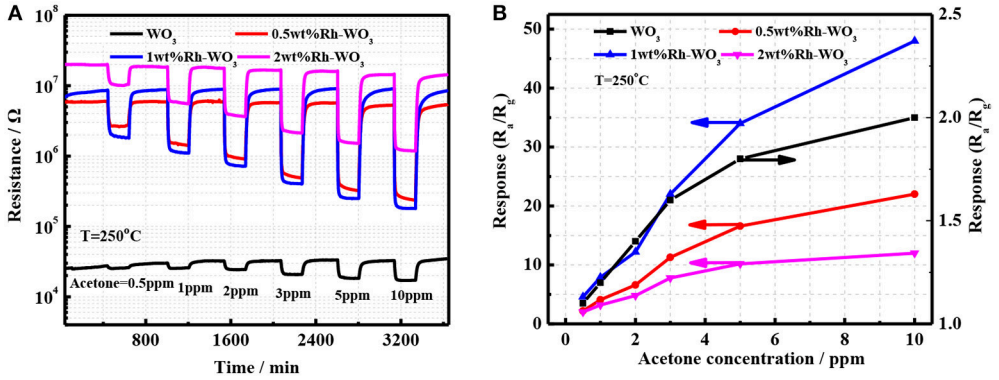

FIGURE 4 | (A) The transient response of four different sensor devices and **(B)** the sensor response as a function of acetone concentration.

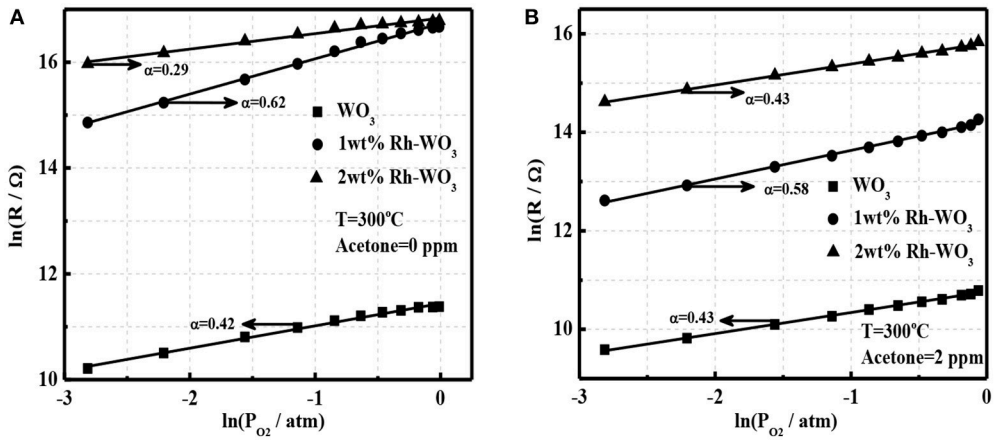

FIGURE 5 | The power-law response to oxygen for pristine WO_3 and Rh-WO_3 **(A)** in the absence of acetone and **(B)** in the presence of 2 ppm acetone at 300°C.

resistance. It was worth noting that the introduction of Rh greatly increased the sensor resistance of WO_3. For 2wt.% Rh-WO_3, the sensor resistance was almost three orders of pristine one. This indicated a strong electronic interaction between Rh_2O_3 and WO_3 surface, forming the well-known P-N junction or fermi-level control sensitization mechanism. Due to the electronic junction of Rh_2O_3 with WO_3, the sensors response and responding speed were significantly promoted. **Figure 4B** shows the calibration line of sensors resistance with concentration of acetone at an operation temperature of 250°C. It was found that sensor based on 1wt.%Rh-WO_3 also responded to 0.5 ppm acetone. One can see that sensor response was increased by 3 times compared with the neat WO_3. However, an excess of Rh did not effectively to promote the sensor response. This observation was in conflict with the great enhancement in sensor resistance. In order to explain the reduction in sensor response for 2wt.%Rh-WO_3, there were two factors should be considered. Firstly, an excessive amount of Rh could lead to agglomeration of Rh_2O_3 and poor dispersion on the surface of WO_3 nanoparticles. Consequently, some electronic interaction of Rh_2O_3 with WO_3 leading to the high resistance were not effective to the sensitization. Secondly, with increasing the amount of Rh the surface activity of WO_3 could be enhanced and then leaded to a catalytic reaction of acetone, which inhibit the diffusion of acetone molecule into inside of sensor films. As a result, the sensor response was reduced by a high loading amount of Rh. This reduction in sensor response could be also observed when increasing operation temperatures. This was evidenced by the strong dependence of sensor response on the operation temperatures for Rh-WO_3 as shown in **Figure S5a**. It was thought that increasing the operating temperature leaded to an enhancement in catalytic activity, which reduces the gas diffusion and sensor response to acetone. When operating at a temperature larger than 250°C, one can note the sensor response greatly decreased with temperatures. It was also found that sensors resistance also obviously decreased with temperature, as shown in **Figure S5b**. For pristine WO_3, the sensor response did not change significantly with temperature and exhibited a lower response at different temperatures. This poor response is associated with a weaker oxygen adsorption on WO_3 surface (Zeng et al., 2017). At the same time, the stability of the sensor was also evaluated as shown in **Figures S5c,d**.

It can be seen that Rh-WO_3 nanoparticles can work for a long time at 350°C and has favorable response recovery performance.

It is well-known that oxygen adsorption in the form of O_2^-, O^-, or O^{2-} on the surface serves as the receptor function and determines the sensing ability and mechanism of MOS gas sensors (Hua et al., 2018a). In order to explore the sensitization effect of Rh-WO_3 nanosheets, we analyzed the oxygen adsorption behavior. **Figure 5A** shows a linear plot of sensor resistance (R_g) with the partial pressure of oxygen (P_{O2}) at a double logarithm-scale for pristine and 1wt.% Rh-WO_3 sensors. It was observed that a linear relationship indicating a power-law response within all P_{O2} ranging from 0.06 to 0.99 atm (1 atm = 100% in volume) and the linear fitting coefficients were 0.42 and 0.62 for pristine and Rh-WO_3, respectively. This indicated that the main type of oxygen adsorption was in the form of O^- for both sensors (Hua et al., 2018a,b) at working temperature of 300°C through:

$$O_2 + 2e^- \rightleftarrows 2O^- \quad (1)$$

In case of 2 wt.% Rh-WO_3, the linear plot of $\ln R_g$ with $\ln P_{O2}$ was also valid. Remarkably, the slope, i.e., fitting coefficient was just 0.29, considerably <0.5. However, it was unlikely that a large amount of Rh on the surface could tailor the form of oxygen ionisorption on the surface. The most probably explanation was that with increasing P_{O2} the oxidized state of Rh, which has been limited to be exposed to atmosphere due to the aggregation of particles, was enhanced and then the electronic interaction between Rh_2O_3 and WO_3 surface was promoted. Consequently, new depletion regions formed, leading to an increase in sensor resistance with P_{O2} and a reduction in the fitting coefficient. This has also been observed in our previous Pt-WO_3 sensor (Li et al., 2017).

According to our recent study, it was found that the power-law response of oxygen in the presence of reducing gas such as H_2, CO, and acetone can be used to clarify the basic sensing mechanism of gas sensors (Hua et al., 2018c). **Figure 5B** shows the power-law response of oxygen in the presence of acetone (2 ppm) for pure and Rh-WO_3 sensors. A very good linearity was observed for all sensors indicating that the basic sensing mechanism of acetone could be explained by the oxidation of acetone with oxygen adsorbates by:

$$CH_3COCH_3 + 8O^- \rightarrow 3CO_2 + 3H_2O + 8e^- \quad (2)$$

For simplicity, it was assumed that acetone catalytic reaction was a complete reaction only producing CO_2 and H_2O. However, in fact the oxidation of acetone was rather complex. In addition, it was also found that linear coefficients of the power-law response were all around 0.5, which was consistent with **Figure 5A** and Equation (1). Importantly, for 2wt.%Rh-WO_3, the fitting coefficient significantly raised up compared with that in the absence of acetone. This clearly supported our explanation for the degradation of sensitization effect with large loading amount of Rh and the reduction in the exponent of the power-law response to oxygen. In this respect, we believe that the basic sensitization mechanism of Rh on WO_3 could be ascribed to the electronic interaction between Rh_2O_3 and WO_3 (p-n junction), which was very similar with the fermi-level control model, popular for Pd-SnO_2 sensors (Tang et al., 2015). The key factor to achieve a good sensitization effect highly relies on an elegant dispersion of Rh_2O_3 on WO_3 surface, which can enhance the electronic interaction with WO_3 surface as schematically drawn in **Figure S6**. This finding was similar with the case of Pt and Ru loaded WO_3 nanosheets, however, it was significantly different with Pd and Fe loaded WO_3. For the later one, the chemical sensitization effect of Pd and Fe plays a vital role through the reaction of surface lattice oxygens with reducing gases.

CONCLUSION

In summary, Rh as a noble catalyst was dispersed onto the surface of WO_3 nanosheets through a wet impregnation method. Experimental results indicated that Rh was in a form of oxidized state Rh_2O_3 on WO_3 surface and an excessive amount of Rh can lead to an aggregation of Rh_2O_3 and poor sensitization effect as well. An electronic interaction between Rh_2O_3 and WO_3 surface was evidenced by an extremely high argument in sensor resistance and it was thought that such an electronic was responsible for the observed sensitization effect of Rh loading. To achieve a good sensitization effect, an elegant dispersion of Rh_2O_3 is required, which highly relies on an effective dispersion method and a proper loading amount. Additionally, a power-law response to oxygen was observed for both pristine and Rh-WO_3 in the presence of acetone, which indicts that oxygen adsorption on the surface of WO_3 serves as a basic receptor function.

AUTHOR CONTRIBUTIONS

YL performed the experiments and analyzed the data with help from DH, CT, CZ, and XT. ZH, MW and EL conceived and guided the study. ZQ wrote the manuscript based on experimental data.

FUNDING

This study was supported by the National Natural Science Foundation of China (Grant NO. 61501167) and Natural Science Foundation of Tianjin (Grant NO. 15JCYBJC52100).

SUPPLEMENTARY MATERIAL

The Supplementary Material for this article can be found online at: https://www.frontiersin.org/articles/10.3389/fchem.2018.00385/full#supplementary-material

REFERENCES

Choi, K. I., Hwang, S. J., Dai, Z., Kang, Y. C., and Lee, J. H. (2014). Rh-catalyzed WO_3 with anomalous humidity dependence of gas sensing characteristics. *RSC Adv.* 4, 53130–53136. doi: 10.1039/C4RA06654E

Dupin, J. C., Gonbeau, D., Vinatier, P., and Levasseur, A. (2000). Systematic XPS studies of metal oxides, hydroxides and peroxides. *Phys. Chem. Chem. Phys.* 2, 1319–1324. doi: 10.1039/a908800h

Houtman, C., and Barteau, M. A. (1991). Adsorbed states of acetone and their reactions on rhodium(111) and rhodium(111)-(2.times.2)oxygen surfaces. *J. Phys. Chem.* 95, 3755–3764.

Hua, Z., Li, Y., Zeng, Y., and Wu, Y. (2018a). A theoretical investigation of the power-law response of metal oxide semiconductor gas sensors ?: schottky barrier control. *Sens. Actuators B Chem.* 255, 1911–1919. doi: 10.1016/j.snb.2017.08.206

Hua, Z., Qiu, Z., Li, Y., Zeng, Y., Wu, Y., Tian, X., et al. (2018b). A theoretical investigation of the power-law response of metal oxide semiconductor gas sensors ??: size and shape effects. *Sens. Actuators B Chem.* 255, 3541–3549. doi: 10.1016/j.snb.2017.09.189

Hua, Z., Tian, C., Huang, D., Yuan, W., Zhang, C., Tian, X., et al. (2018c). Power-law response of metal oxide semiconductor gas sensors to oxygen in presence of reducing gases. *Sens. Actuators B Chem.* 267, 510–518. doi: 10.1016/j.snb.2018.04.002

Hübner, M., Simion, C. E., Haensch, A., Barsan, N., and Weimar, U. (2010). CO sensing mechanism with WO_3, based gas sensors. *Sens. Actuators B Chem.* 151, 103–106. doi: 10.3-106.10.1016/j.snb.2010.09.040

Kadir, R. A., Zhang, W., Wang, Y., Ou, J. Z., Wlodarski, W., and O'Mullane, A. P., et al. (2015). Anodized nanoporous WO_3 schottky contact structure for hydrogen and ethanol sensing. *J. Mater. Chem. A* 3, 7994–8001. doi: 10.1039/C4TA06286H

Kanda, K., and Maekawa, T. (2005). Development of a WO_3, thick-film-based sensor for the detection of VOC. *Sens. Actuators B Chem.* 108, 97–101. doi: 10.1016/j.snb.2005.01.038

Kida, T., Nishiyama, A., Yuasa, M., Shimanoe, K., and Yamazoe, N. (2009). Highly sensitive NO_2 sensors using lamellar-structured WO_3 particles prepared by an acidification method. *Sens. Actuators B Chem.* 135, 568–574. doi: 10.1016/j.snb.2008.09.056

Kim, S. J., Hwang, I. S., Na, C. W., Kim, I. D., Kang, Y. C., and Lee, J. H. (2011). Ultrasensitive and selective C_2H_5OH sensors using Rh-loaded In_2O_3 hollow spheres. *J. Mater. Chem.* 21, 18560–18567. doi: 10.1039/C1JM14252F

Kou, X., Xie, N., Chen, F., Wang, T., Guo, L., Wang, C., et al. (2018). Superior acetone gas sensor based on electrospun SnO_2 nanofibers by Rh doping. *Sens. Actuators B Chem.* 256, 861–869. doi: 10.1016/j.snb.2017.10.011

Li, Y., Hua, Z., Wu, Y., Zeng, Y., Qiu, Z., and Tian, X., et al. (2017). Surface modification of Pt-loaded WO_3 nanosheets for acetone sensing application. *Chem. Lett.* 47, 167–170. doi: 10.1246/cl.170990

Li, Y., Hua, Z., Wu, Y., Zeng, Y., Qiu, Z., and Tian, X., et al. (2018). Modified impregnation synthesis of Ru-loaded WO_3, nanoparticles for acetone sensing. *Sens. Actuators B Chem.* 265, 249–256. doi: 10.1016/j.snb.2018.03.037

Natale, C. D., Paolesse, R., Martinelli, E., and Capuano, R. (2014). Solid-state gas sensors for breath analysis: a review. *Anal. Chim. Acta* 824, 1–17. doi: 10.1016/j.aca.2014.03.014

Owen, O. E., Trapp, V. E., Skutches, C. L., Mozzoli, M. A., Hoeldtke, R. D., and Boden,G. A. (1982). Acetone metabolism during diabetic ketoacidosis. *Diabetes* 31, 242–248. doi: 10.2337/diabetes.31.3.242

Righettoni, M., Tricoli, A., and Pratsinis, S. E. (2010). Si: WO_3 sensors for highly selective detection of acetone for easy diagnosis of diabetes by breath analysis. *Anal. Chem.* 82, 3581–3587. doi: 10.1021/ac902695n

Tang, W., Wang, J., Qiao, Q., Liu, Z., and Li, X. (2015). Mechanism for acetone sensing property of Pd-loaded SnO_2, nanofibers prepared by electrospinning: fermi-level effects. *J. Mater. Sci.* 50, 2605–2615. doi: 10.1007/s10853-015-8836-0

Zeng, Y., Hua, Z., Tian, X., Li, Y., Qiu, Z., and Wang, T. (2017). Modified impregnation synthesis of Fe-loaded WO_3 nanosheets and the gas-sensing properties. *Chem. Lett.* 46, 1353–1356. doi: 10.1246/cl.170555

Conflict of Interest Statement: The authors declare that the research was conducted in the absence of any commercial or financial relationships that could be construed as a potential conflict of interest.